Marine and Petroleum Geology 91 (2018) 562–575

Contents lists available at ScienceDirect

Marine and Petroleum Geology

journal homepage: www.elsevier.com/locate/marpetgeo

Research paper

Shelf-edge trajectory and sediment dispersal in a lacustrine setting: A case study from Qinnan Depression, Bohai Bay Basin, China

Shang Xu[a], Fuyun Cong[a,*], Fang Hao[b,a], Changgui Xu[c], Huayao Zou[d,**], Xintao Zhang[c], Shaohua Xu[e]

[a] Key Laboratory of Tectonics and Petroleum Resources, Ministry of Education, China University of Geosciences, Wuhan 430074, China
[b] School of Geosciences, China University of Petroleum, Qingdao 266580, China
[c] Tianjin Branch of China National Offshore Oil Company Ltd, Tianjin 300452, China
[d] State Key Laboratory of Petroleum Resources and Prospecting, China University of Petroleum, Beijing 102249, China
[e] Chongqing Key Laboratory of Complicated Oil and Gas Field Exploration and Development, Chongqing University of Science and Technology, Chongqing 401331, China

ARTICLE INFO

Keywords:
Shelf-edge trajectory
Sediment dispersal
Lacustrine basin
Tectonic subsidence
Lateral variability
Sediment supply

ABSTRACT

The Oligocene succession of Dongying Formation in Qinnan depression in Bohai Bay Basin has preserved well-imaged lacustrine prograding shelf-edge scale clinoforms, providing a good opportunity to study the relationship between shelf-edge trajectory, stratal stacking patterns and sediment dispersal, and to investigate the effect of controlling factors on sediment dispersal shelf-edge trajectories in a lacustrine setting. 3D seismic volumes were used for defining seismic units, bounding surfaces, shelf-edge trajectories and sediment dispersal. Four seismic units have been subdivided, and four types of shelf-edge trajectories and the associated stratal stacking patterns have been recognized. Greater volume of sandstone in deep-water area tends to develop in seismic units with descending shelf-edge trajectory angles and tends be linked to lower shelf-edge trajectory angles. Differential tectonic subsidence rates along the shelf and along-strike variation in sediment supply were prime factors controlling lateral variability in trajectory, progradation and sediment dispersal. The evolution of shelf-edge trajectory can be subdivided into three stages. Local climate might play a major role in controlling lake-margin evolution during the first two stages, when dry hot weather foster basin floor fan deposition and descending trajectories, and humid cold weather hindered the development of basin floor fan and forms ascending trajectories. While differential tectonic subsidence could have the dominate role during the third stage, when climate signal can hardly be recognized and lateral variability in trajectory angles and sediment supply is most obvious.

1. Introduction

The concept of 'Trajectory analysis' was introduced by Helland-Hansen and Martinsen (1996), and was considered as a model-independent descriptive tool for stratigraphic analysis (Catuneanu et al., 2009; Helland-Hansen and Hampson, 2009; Henriksen et al., 2009). Shelf-edge trajectory analysis is the study of vertical and lateral migration patterns of shelf edges and associated shelf, slope and basin-floor systems. 'Shelf', 'Slope', 'Basin floor' and 'Shelf-edge' are used as process-oriented terms to describe the according segments of large-scale clinoforms which have an amplitude of 100–1000 m at most types of basin, but not restricted to the sedimentary prism built on passive continental margins (Steel and Olsen, 2002; Helland-Hansen and Hampson, 2009).

By investigating the coupling of shelf-edge trajectories, stratal stacking patterns, dynamic analysis of sediment fluxes and partitioning from shallow to deep water areas can be achieved, and precise prediction of lithologies and deep-water sedimentation can be realized (Helland-Hansen and Gjelberg, 1994; Helland-Hansen and Martinsen, 1996; Mellere et al., 2002; Steel and Olsen, 2002; Helland-Hansen and Hampson, 2009, Bullimore and Helland-Hansen, 2009; Henriksen et al., 2009, 2011; Gong et al., 2015a, 2015b). Early stratigraphic models suggested that large-scale basin-floor fans tended to be associated with descending of flat trajectories (Steel et al., 2000; Steel and Olsen, 2002; Mellere et al., 2002; Johannessen and Steel, 2005; Petter and Steel, 2006; Ryan et al., 2009). Along with the development of shelf-edge trajectory theory, different relationships between shelf-edge trajectories and deep-water sedimentation systems have been reported. The effects of sediment supply (Bullimore et al., 2008; Bullimore and Helland-Hansen, 2009; Steel et al., 2008; Carvajal and Steel, 2006; Carvajal

* Corresponding author. Key Laboratory of Tectonics and Petroleum Resources, Ministry of Education, China University of Geosciences, Lumo Road No.388, Wuhan 430074, China.
** State Key Laboratory of Petroleum Resources and Prospecting, China University of Petroleum, 18 Fuxue Road, Changping District, Beijing 102249, China.
E-mail addresses: fuyuncong@hotmail.com (F. Cong), huayaozou@cup.edu.cn (H. Zou).

https://doi.org/10.1016/j.marpetgeo.2018.01.027
Received 17 July 2017; Received in revised form 21 December 2017; Accepted 21 January 2018
Available online 03 February 2018
0264-8172/ © 2018 Elsevier Ltd. All rights reserved.

et al., 2009), climate conditions (Muto and Steel, 1997; Muto et al., 2007; Kertznus and Kneller, 2009; Gong et al., 2016a), process regimes at the shelf edge (Johannessen and Steel, 2005; Dixon et al., 2012; Gong et al., 2016b) and lateral variability in accommodation/supply conditions (Henriksen et al., 2009; Olariu and Steel, 2009; Dixon et al., 2012; Santra et al., 2013; Bourget et al., 2014; Jones et al., 2015) on sediment dispersal have been discussed by many researchers.

Currently most research on shelf-edge trajectories and sediment dispersal are focusing on marine settings. Hydrologically closed or semi-closed lacustrine settings have received comparatively very little attentions. Previous studies on lacustrine settings could only be found in Pannonian basin (Uhrin and Sztanó, 2011; Sztanó et al., 2013) and Dacian basin (Munteanu et al., 2012; Fongngern et al., 2015). The factors driving the formation of shelf-edge trajectory and sediment dispersal are quite different in lacustrine basins compared with those in marine basins, specifically, lake types (i.e. underfilled lake, balanced lake and overfilled lake types of Carroll and Bohacs, 1999), local climate variations (shown as the amount of precipitation and evaporation) and tectonic subsidence have been emphasized by previous studies to have direct controls on sediment dispersal, relative lake level and subsequent shelf-edge trajectories (Carroll and Bohacs, 1999; Sztanó et al., 2013; Uhrin and Sztanó, 2011; Fongngern et al., 2015). For example, Sztanó et al. (2013) highlighted that local cyclic climate changes, rather than global sea-level changes, controlled base-level, water volume and composition of sediment arriving to the Pannonian lake basin; Fongngern et al. (2015) noticed that local differential tectonic movement could cause relative lake level change along the basin margin and subsequent variation in shelf-edge trajectory patterns in Darcian lake basin. Unraveling the interplay between shelf-edge trajectories and sandstone configuration will be of great help to explore the hydrocarbon reservoirs in lacustrine basins.

Bohai Bay basin is a Cenozoic continental lacustrine basin in North China. The Oligocene succession of Dongying Formation in Qinnan Depression in Bohai Bay basin has a well-imaged succession of prograding shelf-edge scale deltaic clinoforms with relief of 100–300 m. It provides a good opportunity to study the relationship between shelf-edge trajectories, stratal stacking patterns and sediment dispersal, and to investigate the effect of external factors such as tectonic subsidence and climate variation on sediment dispersal and shelf-edge trajectories in a lacustrine setting.

2. Geological settings

The Bohai Bay Basin, with an area of about 180,000 km^2 and located on the eastern coast of China (Fig. 1A), is one of the most important petroleum basins in China. The Bohai Bay Basin formed on the top of the North China Craton and had a complex geological history (Wang and Qian, 1992; Ge and Chen, 1993; Huang and Pearson, 1999; Hou et al., 2001). This basin developed as a back-arc basin during the Mesozoic and evolved into an intracratonic rift basin during the Cenozoic (Huang and Pearson, 1999; Hao et al., 2009).

The Qinnan Depression is located in the northwest side of Bohai Sea and covers an area of 2300 km^2 in an East-West direction, and it is one of the least explored depressions in Bohai Bay basin (Lai et al., 2007; Shi et al., 2014). The depression is bounded by the Matouying uplift to the west, the Liaoxi uplift to the east, the Qinnan uplift to the south and the Shijiutuo uplift to the south. Within the Qinnan Depression, syndepositional normal faults I and II further subdivide the Depression into western sag, central sag, eastern sag and northeastern sag, among which the eastern sag is the largest (Fig. 1B) (Shi et al., 2014).

Qinnan Depression has experienced two evolutional stages: Paleogene syn-rift stage and Neogene post-rift stage. The synrift sequence contains the Paleogene Kongdian, Shahejie and Dongying formations that were deposited primarily in lacustrine environments. The postrift sequence includes the Neogene Guantao, Minhuazhen and Pingyuan formations that were deposited primarily in fluvial environments (Fig. 2). In synrift stage, the evolution of rift basin and the distribution of sedimentary systems are controlled by the periodic activity of normal faults (Lai et al., 2007; Shi et al., 2014). During the Oligocene Dongying formation, sediments were mainly supplied by the adjacent uplifts, and large braided delta developed on the sloping areas (Shi et al., 2014).

3. Data and methods

3.1. Seismic analysis and interpretation

The study area is located in the eastern sag of Qinnan Depression (Fig. 1B). 3D seismic volumes were used for defining seismic units and bounding surfaces. The 3D seismic data used in this study was provided by the Tianjin branch of the China National Offshore Oil Corporation Ltd. The seismic data is a 30 km × 36 km rectangular survey that covers the major depocenter of the eastern sag of Qinnan depression (Fig. 3). The data are zero phase and displayed by using SEG polarity convention, which depicts black reflections as positive and red reflections as negative. The dominant frequency in the Paleogene interval is 28–30 Hz. The average velocity value of 2000 m/s for Dongying Formation was suggested by Xu et al. (2015, 2016). As no well penetrating into the studied interval, two-way travel time is used to present vertical depth measurement on seismic lines.

Eight dip-oriented cross-sections were used for interpretation (Fig. 3). The T2 and T3 regional unconformities were recognized to be the boundaries of Eocen Shahejie Formation, Oligocene Dongying Formation and Miocene Guantao Formation (Hao et al., 2009; Xu et al., 2014, Fig. 2), respectively. Thus the study interval is believed to be Oligocene Dongying Formation (Fig. 4). As biostratigraphy and age control are not sufficient, subdivision of the study interval was not conducted.

Root-mean-square (RMS) amplitude maps were extracted from the bounding surfaces of seismic units, and they were used for lithofacies identification. Time isochore maps based on the vertical two-way time (TWT) of seismic units are used for depocenter identification.

All of our seismic profiles are undecompacted. Deibert et al. (2003) and Petter et al. (2013) suggest that differential compaction leads to a decrease in gradients and heights of clinothems, but that different sediment loading causes gradients and heights of clinothems to increase. The effects of differential compaction and loading, therefore, tend to balance each other out (Deibert et al., 2003; Petter et al., 2013), indicating that our trajectory trends measured from undecompacted cross-sections are similar to those inferred from decompacted seismic profiles. Carvajal and Steel (2006), and Gong et al. (2015a, 2015b, 2016a) also have shown that little difference in trajectory trends and clinoform dimensions exists between restored and non-restored clinothem geometries.

3.2. Quantitative parameters

Several quantitative parameters were measured on cross-sections and RMS maps in Figs. 4–7 to describe shelf-edge trajectories, stratal stacking patterns, sediment dispersal patterns and volume of deep-water sandstone. Progradation distances (P), maximum thickness of topsets (MT_t) and bottomsets (MT_b), forest dip (D_f), clinoform height (H_c), shelf-edge trajectory angles (T_{se}) and differential sedimentation on shelf and basin (As/Ab) were measured directly on cross-sections as suggested by Salazar et al. (2015) and Gong et al. (2015a, 2015b, 2016a), and were summarized in Tables 1 and 2.

Sandstone trajectories and sandstone width (W_s) are developed in this paper as new parameters to reflect sandy sediment dispersal patterns and volume of deep-water sandstone respectively, and they were measured on each RMS attribute maps. Sandstone trajectories represent the basinward boundary of sandy deposits at the end of each seismic unit, and can be used to discuss the sediment dispersal patterns.

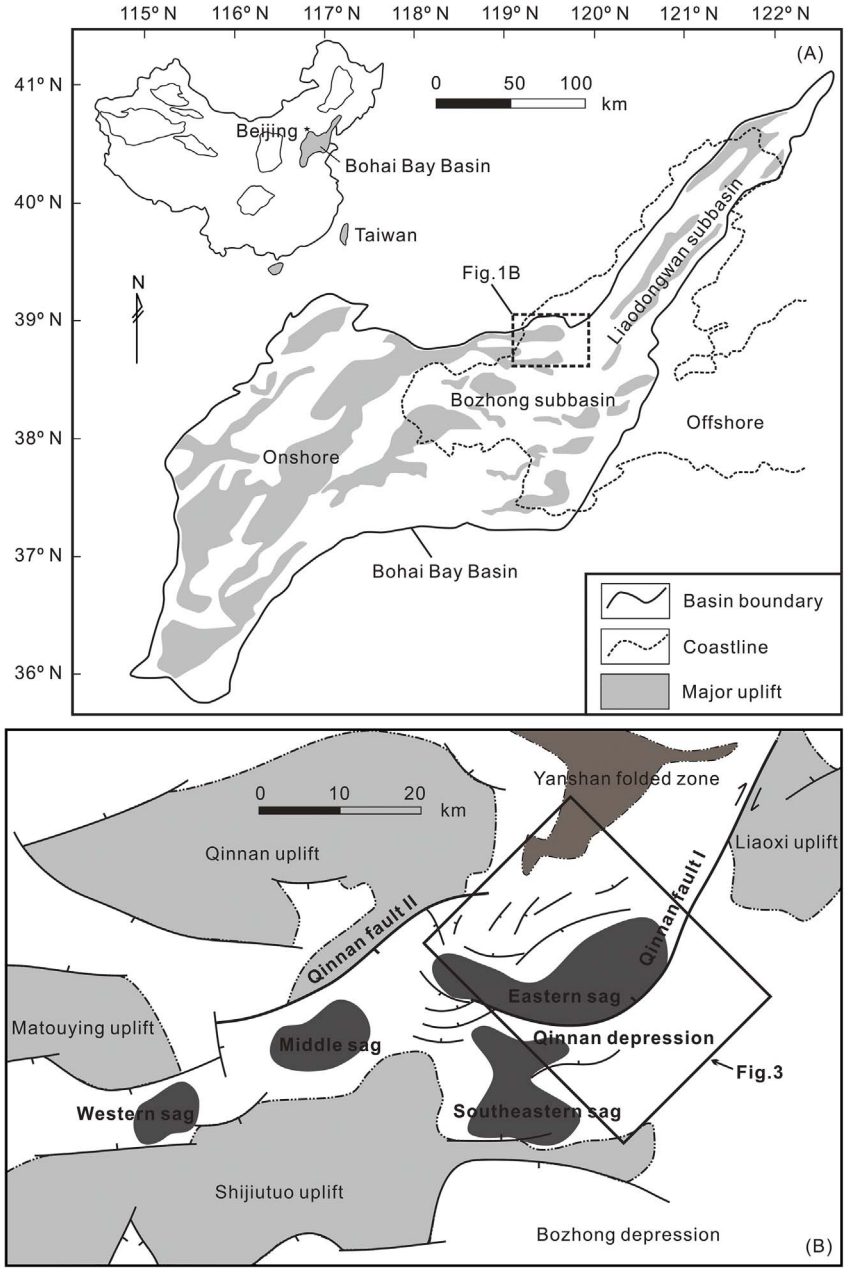

Fig. 1. (A) Sub-basins of the Bohai Bay Basin (modified from Hao et al., 2007). (B) Locations of the study area in the Qinnan depression.

Sandstone width represents the dip-oriented width of sandy fans in the RMS attribute maps, and can be used to discuss the volume of deep-water sandstone if combining with other parameters like maximum thickness of bottomsets.

4. Results

4.1. Seismic units and bounding surfaces

The Oligocene Dongying formation successions within Qinnan Depression have been subdivided into four units, namely Seismic Unit 1 (SU1), Seismic Unit 2 (SU2), Seismic Unit 3 (SU3) and Seismic Unit 4 (SU4), respectively. The seismic units are bounded by bounding surfaces 1–5, and they record the changes in shelf edge trajectories, stratal stacking patterns and sediment dispersal along shelf to basin floor (Figs. 5 and 6).

4.1.1. Bounding surface 1 and seismic unit 1

Bounding surface 1 constitutes the base of SU1, and is characterized by a fairly smooth profile in dip-oriented sections. This surface marks the initiation of clinoform growth, as indicated by the development of topsets and foresets and clearly recognizable steepening of slope gradient on the overlying seismic unit. The seismic reflections on the topset and foreset display low amplitude character, while seismic reflections the bottomset display high amplitude reflections (Figs. 5 and 6). The RMS amplitude attribute map of bounding surface 1 reveals high-amplitude distribution on the bottomset mainly in the southern region and low-amplitude distribution on the topset and foreset (Fig. 7A).

Seismic Unit 1 is bounded by bounding surface 1 and 2 (Figs. 5 and 6). The time isochore map extracted from seismic unit 1 shows the main depocenter locates on the foreset, with the thickest part in the northeast region (Fig. 8B).

Individual clinothems in Seismic Unit 1 display very thin topset and thick foreset and bottomset. The maximum thickness of topsets (MT_t) is nearly zero, and the range in maximum thickness of bottomsets (MTb)

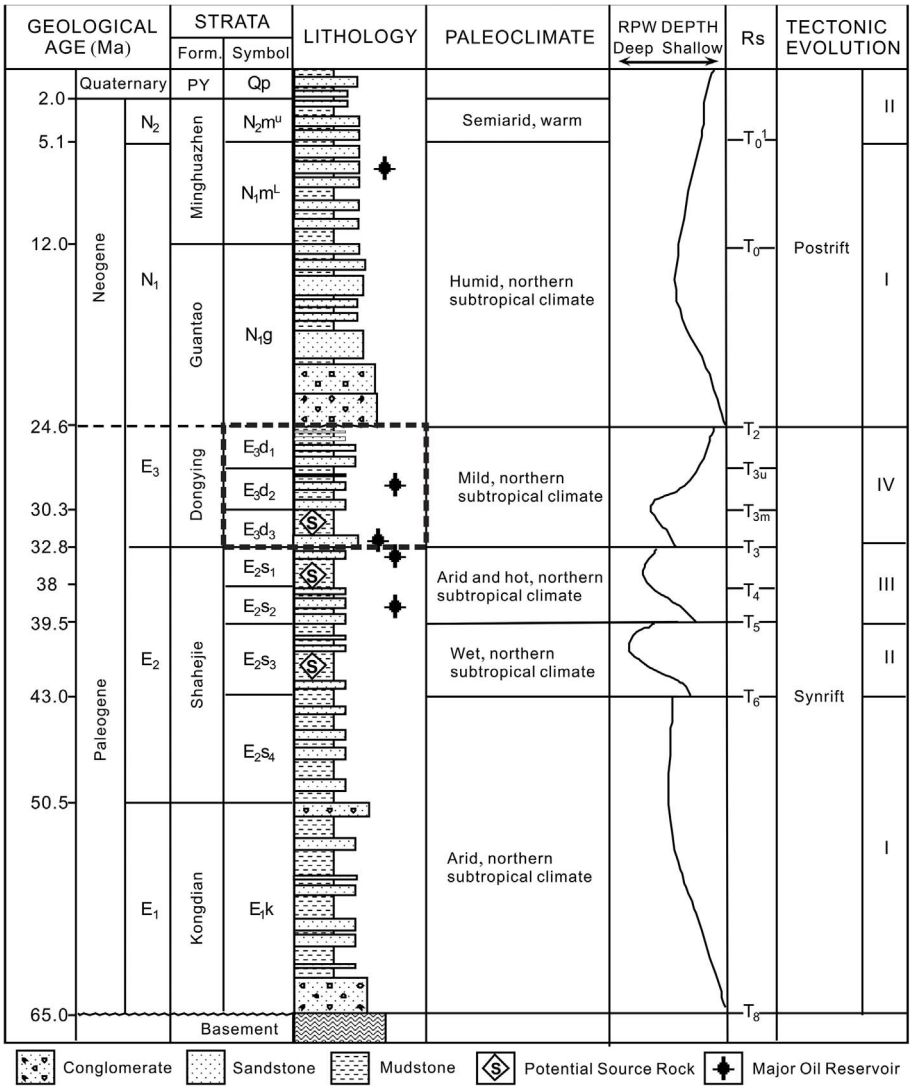

Fig. 2. Generalized stratigraphy of the Bohai Bay basin (modified from Hao et al., 2009; Xu et al., 2014). The study interval is marked by dashed line. Form: Formation; PY: Pingyuan; RPW Depth: relative palaeo-water depth.

is 71.27–104.82 ms (Table 2). Seismic facies were determined throughout the seismic units as areas with particular amplitude and lateral continuity characteristics (John et al., 2005; Kertznus and Kneller, 2009). Seismic facies within SU1 consists of oblique clinoform seismic faices with moderate to high amplitude reflections, the ranges of clinoform height (H_c) and forest dip (D_f) are 77.63–150.44 ms and 14–17°, respectively (Table 1). Laterally continuous high amplitude parallel reflections on the toe of slope and basin floor and low amplitude discontinuous chaotic reflections on the slope. (Figs. 5 and 6).

4.1.2. Bounding surface 2 and seismic unit 2

The RMS amplitude attribute map of bounding surface 2 shows strike elongate broad ribbon-shaped high amplitude distribution on the bottomset mainly in the southwest region, and narrow medium-high amplitude distribution on the bottomset in the northeast region (Fig. 7B).

Seismic Unit 2 is bounded by bounding surface 2 and 3. Although the main depocenter still locates on the foreset, the thickest part has shifted from the northeast region to the southwest region (Fig. 8C). Individual Clinothems in Seismic Unit 2 display thicker topset and foreset and thinner bottomset than SU1 (Figs. 5 and 6). The ranges of maximum thickness of topsets (MT_t) and bottomsets (MT_b) are 36.62–60.31 ms and 55.04–86.84 ms, respectively (Table 2).

Seismic facies in SU2 consist of sigmoidal clinoform seismic facies. The ranges of clinoform height (H_c) and forest dip (D_f) are 57.46–106.58 ms and 12–19°, respectively (Table 1). Low amplitude chaotic and transparent facies can be observed on the shelf and upper slope within the seismic unit, and high amplitude parallel reflections can be observed on the lower part of the slope and basin floor (Figs. 5 and 6).

4.1.3. Bounding surface 3 and seismic unit 3

The RMS amplitude attribute map of bounding surface 3 shows narrow medium-to high-amplitude strike elongate thread-shaped distribution on most areas of the bottomset and high amplitude lobate-shaped deposits on the bottomset in the northeast corner (Fig. 7C).

Seismic Unit 3 is bounded by bounding surface 3 and 4. As revealed by time isochore map, the foreset is still the depocenter, but the thickness of the forest along the strike is much more uniform than SU1 and SU2 (Fig. 8D). Individual clinothems in Seismic Unit 2 show much thicker topset, foreset and bottomset than that of SU1 and SU2 (Figs. 5 and 6). The ranges of maximum thickness of topsets (MT_t) and bottomsets (MT_b) are 59.65–100.66 ms and 92.98–112.50 ms, respectively (Table 2).

Seismic facies in SU3 consist of sigmoidal clinoform seismic facies. The ranges of clinoform height (H_c) and forest dip (D_f) are 54.39–108.55 ms and 9–18°, respectively (Table 1). In the southwest region where angles of the shelf-edge trajectory are steeper, high amplitude reflections distribute on the foreset and bottomset. While in the northeast region where angles of the shelf-edge trajectory are smoother,

Fig. 3. Location of the study area in eastern sag of Qinnan depression and the location of seismic cross-lines. Major fault zone 1 and 2 and associated secondary faults are also shown.

the high amplitude reflections mainly distribute on the bottomset (Figs. 5 and 6).

4.1.4. Bounding surface 4 and seismic unit 4

The RMS amplitude attribute map of bounding surface 4 shows narrow medium-to high-amplitude strike elongate ribbon-shaped deposits on the bottomset with relatively uniform width from southwest to north east (Fig. 7D).

Seismic Unit 4 is bounded by bounding surface 4 and 5, and is characterized by sigmoidal clinoform seismic facies. The ranges of maximum thickness of topsets (MT_t) and bottomsets (MT_b) are 29.82–36.62 ms and 39.04–66.45 ms, respectively (Table 2). The depocenter locates on the lower foreset and bottomset, with the thickest part in the southwest region (Fig. 8E). The ranges of clinoform height (H_c) and forest dip (D_f) are 30.48–62.06 ms and 7–15°, respectively (Table 1).

4.1.5. Bounding surface 5

Bounding Surface 5 is characterized by a smooth profile, with gentle slope gradient (Figs. 5 and 6). As the 3D seismic data only covers the shelf and slope area of seismic unit 4, the RMS amplitude attribute map of bounding surface 5 shows high amplitude distribution in the central region and the southwest corner (Fig. 7E).

4.2. Seismic facies interpretation and lithological prediction

Seismic facies analysis and interpretation from SU1 to SU4 was carried out following the classical procedures described by Mitchum et al. (1977).

Oblique and sigmoidal clinoform facies are characteristic of moderate-to high-amplitude seismic reflections, and show obvious topset, foreset and bottomset. Spatial variations in amplitude along the depositional profile can be observed in oblique and sigmoidal clinoform facies as a result of the distribution of varying grain sizes (hence

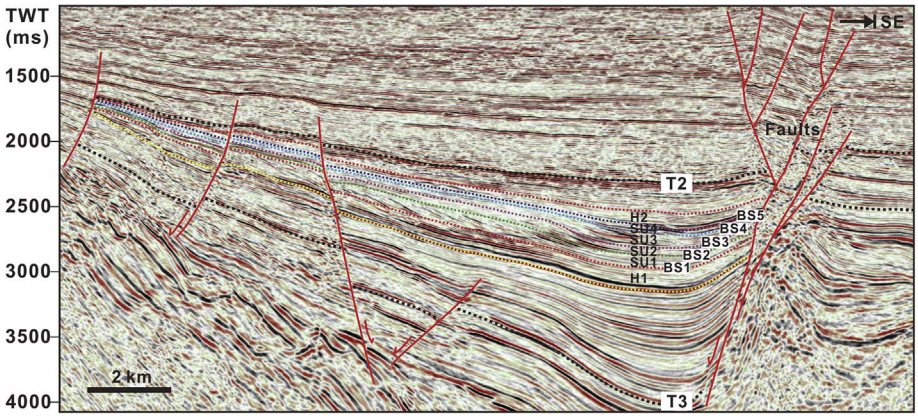

Fig. 4. A regional depositional dip-oriented cross-section in the center of the study area showing the stratigraphic and structural architecture of the study area. The location of the cross-section is shown in Fig. 3. Note that the vertical scale is in two-way-time (TWT). The intervals (H1, SU1, SU2, SU3, SU4 and H2) selected for time isochore map extraction are also shown.

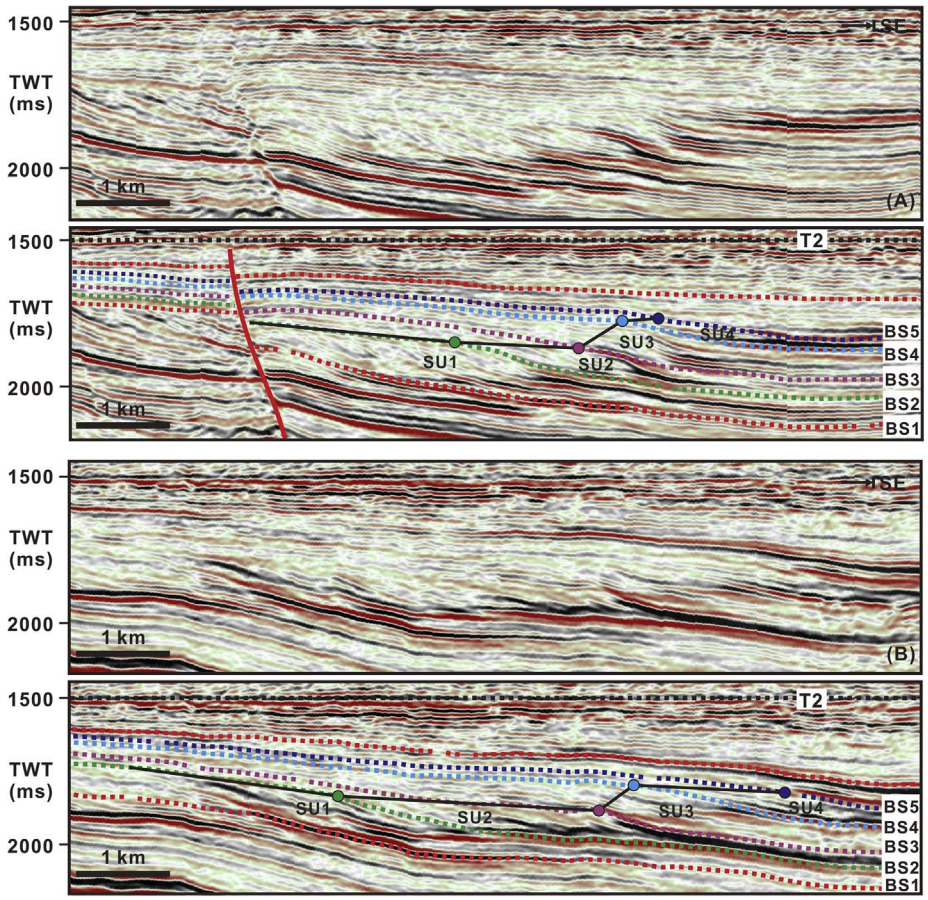

Fig. 5. Two uninterpreted and interpreted depositional dip-oriented cross-sections. (A) Uninterpreted cross-section Line 7 in the southwest; interpreted cross-section Line 7 in the southwest; (B) uninterpreted cross-section Line 1 in the northeast. Interpreted cross-section Line 1 in the southwest. The location of the cross-sections are shown in Fig. 3. Note the cross-sections are flattened on T2. Stark differences in progradation distances and shelf-edge trajectory angles can be obseed, especially in seismic unit 2 (bounded by BS2 and BS3) and seismic unit 4 (bounded by BS4 and BS5).

acoustic impedance).

Laterally continuous high amplitude parallel reflections can be observed on the toe of slope and basin floor. The high amplitude reflections are highly aggradational and are sub-horizontal and horizontal. This seismic facies is generally interpreted as basin-floor fan deposits with sandier sediments than the overlying and underlying deposits.

Low amplitude to transparent and chaotic facies can also be observed on the shelf and slope. Low amplitude to transparent facies comprises of laterally sub-continuous, sub-horizontal reflections. Due to the low acoustic impedance, the presence of transparent facies is interpreted in some cases as fine-grained turbidity currents (Fongngern et al., 2015), and in others as packages of stratal with uniform lithological content (Kertznus and Kneller, 2009). Low amplitude chaotic facies comprises of discontinuous and disorganized reflections. The difference in reflectivity and continuity is likely the result of variable sand content in dominantly muddy sections (Kertznus and Kneller, 2009), and in some cased interpreted as mass transport deposits.

Lithological distribution and prediction in map view can be described by RMS amplitude attribute maps. As seen in Fig. 7, RMS amplitude attribute maps of bounding surfaces show medium-to high-amplitude values mainly on the bottomset. Considering the distribution of high-amplitude RMS values correspond to the continuous high amplitude parallel seismic reflections underlying the bounding surfaces, we interpret medium-to high-amplitude RMS values as sandy basin-floor fans, similar to the interpretation in another case study in Bohai bay basin carried out by Xu et al. (2014). However it is important to highlight that these lithological interpretation and predictions are highly speculative given no wells penetrating into the studied intervals that are available for calibration within the study area.

4.3. Lacustrine shelf-edge trajectory and stratal stacking patterns

Before identifying shelf-edge trajectory, the cross-sections were flattened on horizon T2 whose geometry appeared to be relatively flat throughout the data set and thus assumed was deposited close to horizontal. Following the concepts developed by Helland-Hansen and Gjelberg (1994), Helland-Hansen and Martinsen (1996) and Helland-Hansen and Hampson (2009) for trajectory analysis, shelf-edge trajectories were plotted on eight flattened dip-oriented seismic profiles (Figs. 5 and 6) and the associated progradation distances of each seismic unit were calculated for comparison (Table 1). The migration patterns of shelf edge and the sandstone trajectory were shown in a map view (Figs. 7 and 9).

Four types of shelf-edge trajectories and the associated stratal stacking patterns can be recognized: (1) Steeply descending trajectory with progradational and downstepping stratal stacking patterns; (2) Slightly descending to flat trajectory with aggradational and progradational stratal stacking patterns; (3) Slightly ascending trajectory with aggradational and progradational stratal stacking pattern; (4) Steeply ascending trajectory with aggradational and progradational stratal stacking patterns (Figs. 5 and 6). Different types of shelf-edge trajectories reflect different relative lake level trends: steeply descending trajectories indicate long term relative lake level fall, slightly descending to flat trajectories indicate falling or stable relative lake level, and ascending trajectories indicate relative lake level rise (Steel and Olsen, 2002; Johannessen and Steel, 2005; Helland-Hansen and Hampson, 2009).

Steeply descending trajectory with negative trajectory angles ($-10^{\circ}\sim -5^{\circ}$) and progradational and downstepping stratal stacking patterns have been observed in SU1. Clinothems prograded and downstepped in the basinward direction, characterized by oblique clinoform seismic facies (Figs. 5 and 6). The value of differential

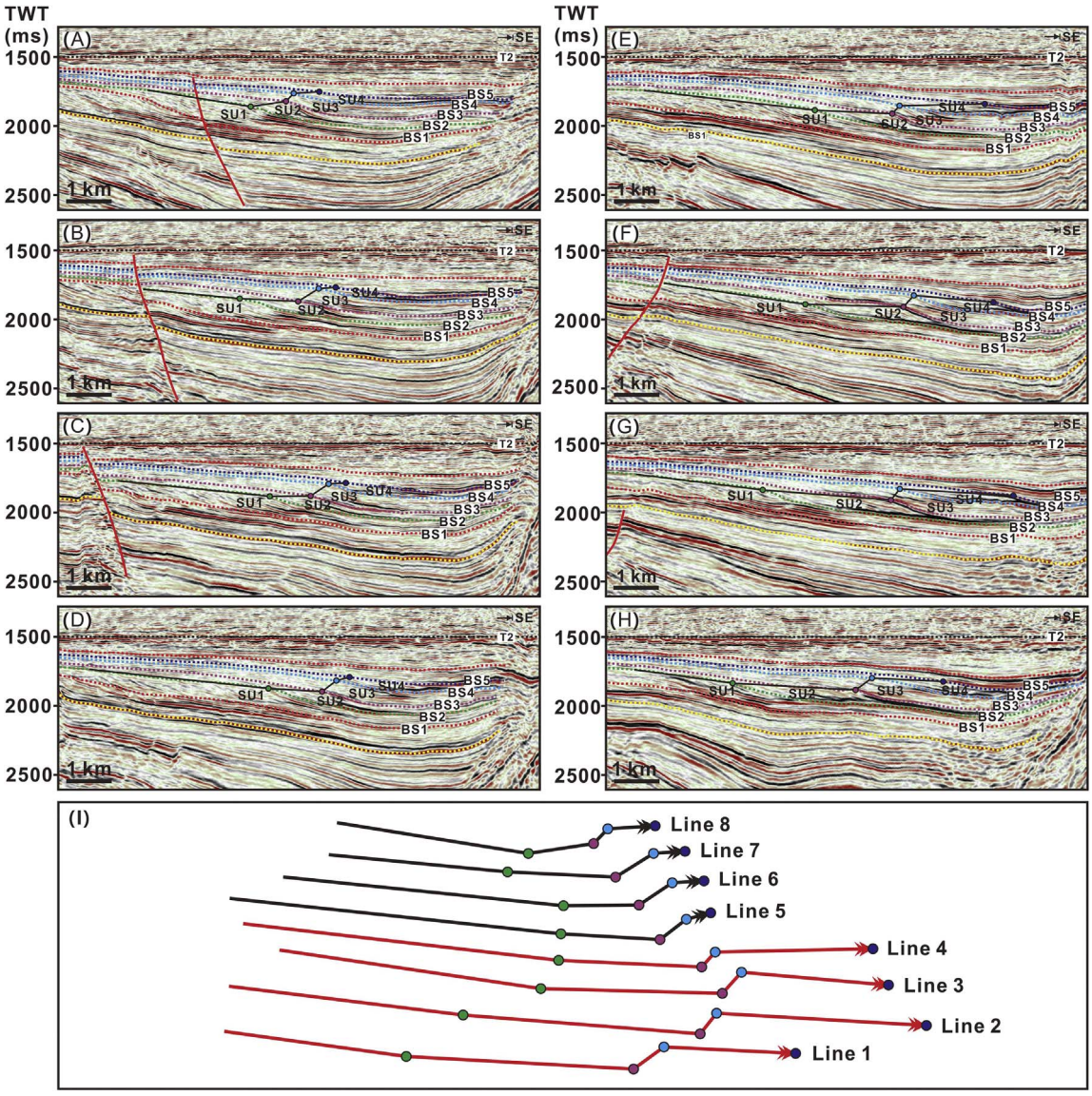

Fig. 6. Interpreted depositional dip-oriented cross-sections from northeast to southwest and shelf-edge trajectories. The locations of the cross-sections are shown in Fig. 3. (A) Line 8; (B) Line 7; (C) Line 6; (D) Line 5; (E) Line 4; (F) Line 3; (G) Line 2; (H) Line 1; (I) Shelf-edge trajectories and shelf-edge rollovers for four seismic units extracted from eight seismic cross-sections. Note the cross-sections are flattened on T2.

sedimentation on shelf and basin (As/Ab) is nearly zero (Table 2).

Slightly descending to flat trajectory with negative trajectory angles ($-5^{\circ} \sim 0^{\circ}$) with aggradational and progradational stratal stacking patterns have been observed in SU2 and part of SU4. Clinothems prograded and aggredaded in the basinward direction, characterized by sigmoid clinoform seismic facies (Figs. 5 and 6). Range in progradational distances (P) and differential sedimentation on shelf and basin (As/Ab) for SU2 are 0.80–2.78 km and 0.63–1.02, respectively (Tables 1 and 2).

Steeply ascending trajectory with positive trajectory angels ($> 10^{\circ}$) and aggradational and progradational stratal stacking patterns have been observed in SU3. Clinothems show dominantly aggredational stacking patterns, characterized by sigmoidal clinoform seismic facies (Figs. 5 and 6). Range in progradational distances (P) and differential sedimentation on shelf and basin (As/Ab) for SU3 are 0.17–0.37 km and 0.62–1.05, respectively (Tables 1 and 2).

While it is worth to be noted that, both slightly ascending trajectory with positive trajectory angles (0°–10°) and slightly descending to flat trajectory with negative trajectory angles ($-5^{\circ} \sim 0^{\circ}$) coexist in SU4, with the northeast parts showing low-angle ascending trajectories and the southwest parts showing descending to flat trajectories (Figs. 5 and 6; Table 1). In each type of trajectory regimes, clinothems show aggradational and progradational stratal stacking pattern, characterized by sigmoidal clinoform seismic facies. Range in progradational distances (P) and differential sedimentation on shelf and basin (As/Ab) for SU4 are 0.58–2.57 km and 0.52–0.94, respectively (Tables 1 and 2).

4.4. Variation in progradation and sandstone width

Comparing different Seismic Units, greater shelf-edge progradation distances tend to be observed during descending and flat trajectories than in ascending trajectories (Figs. 6 and 10). Within single Seismic Unit, progradation distances also have negative correlations with trajectory angles (Fig. 10; Table 1). Along-strike variation in progradation distances and trajectory angles can be seen in Seismic Unit 2 and 4. As presented in Table 1, from northeast to southwest region in SU2 and SU4, progradation distances increase and trajectory angles decrease regularly. Possible explanations for this along-strike variation are discussed later.

The relationship between progradation distances and sandstone

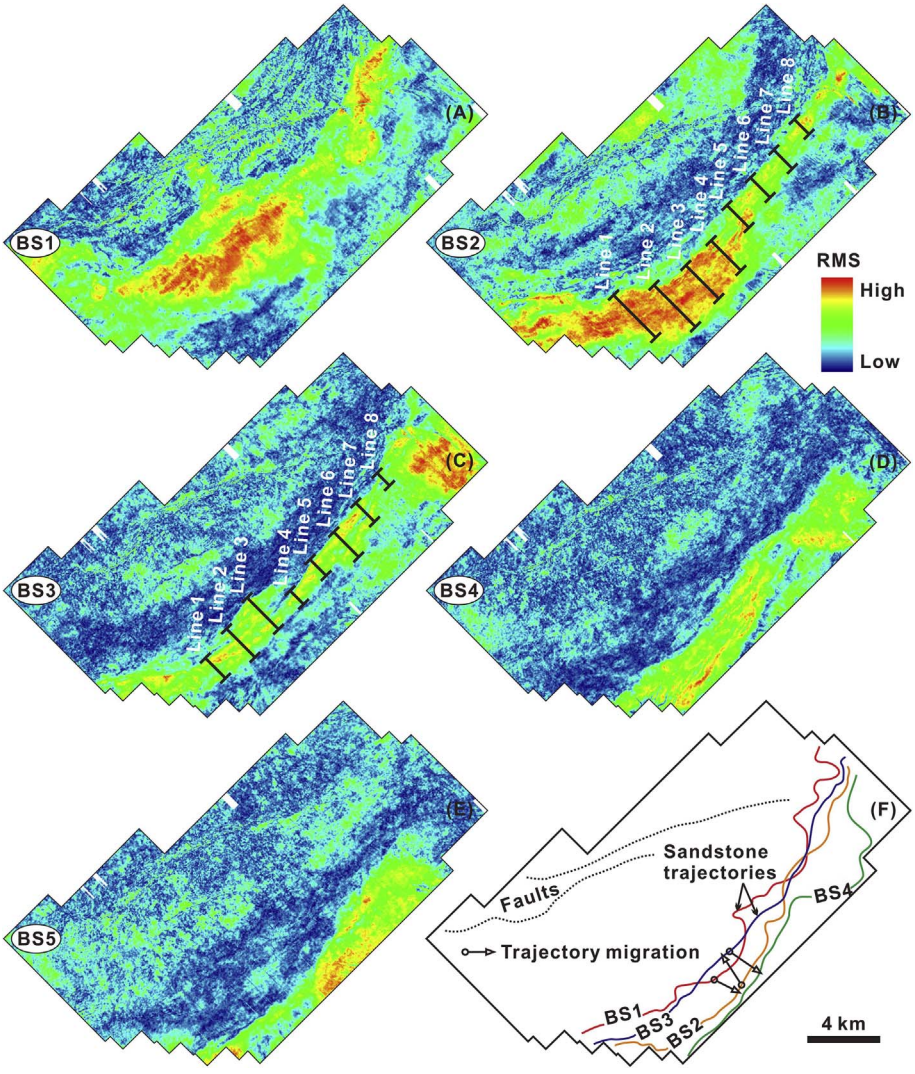

Fig. 7. RMS Attribute maps of bounding surfaces representing the lithology distribution and sandy fan deposition in each seismic units. (A–E): RMS Attribute map extracted from BS1 to BS5. The map view of sandstone trajectories (BS1-4) are depicted by tracking the near-slope edges of sandy fans.

width was investigated in SU2 with slightly descending trajectory and in SU3 with steeply ascending trajectory (Figs. 7 and 10). As shown in Fig. 10, in SU2 with descending trajectories, clear positive correlations between progradation distances and sandstone width and negative correlation between shelf-edge trajectory angles and sandstone width can be seen. Although a small area of sandstone formed in SU3 with ascending trajectories, no clear correlation between progradation distances and sandstone width exists. Collectively, values of sandstone width are bigger in Seismic Units with descending trajectories than in Seismic Units with ascending trajectories.

5. Discussion

5.1. Linking shelf-edge trajectories and stratal stacking patterns to sandy sediments dispersal patterns and volume of deep-water sandstone

This discussion uses measured sandstone trajectory and sandstone width in map view, shelf-edge trajectory angles and progradation distances of each seismic unit to develop a relationship between shelf-edge trajectories, stratal stacking patterns and sediment dispersal patterns and volume of deep-water sandstone.

Table 1
Measured progradation distances, trajectory angles, and foreset dip and clinoform height for Seismic Units 1 to 4. Greater progradation distances are associated with lower trajectory angles. Note within SU2 and SU4 lateral variability in progradation distances and trajectory angles exist. Especially in SU4 where ascending and descending shelf-edge trajectories co-exist and angles tend to decrease from northeast to southwest (Line 8 to Line 1). P - progradation distances, T_{se} - shelf-edge trajectory angles, D_f - foreset dip, H_c - clinoform height.

Cross-Lines	P (km)			T_{se} (°)				D_f (°)				H_c (ms)			
	SU2	SU3	SU4	SU1	SU2	SU3	SU4	SU1	SU2	SU3	SU4	SU1	SU2	SU3	SU4
8	0.80	0.18	0.58	−9	9	46	4	15	19	12	8	77.63	74.56	54.39	31.14
7	1.32	0.47	0.38	−5	−3	32	4	14	12	12	8	117.11	73.68	82.02	62.06
6	0.92	0.41	0.39	−6	0	34	3	17	16	18	8	54.61	57.46	61.62	35.75
5	1.21	0.33	0.30	−6	−3	38	7	16	16	11	7	100.66	85.31	61.18	42.76
4	1.75	0.17	1.93	−7	−2	47	1	14	18	9	8	150.44	93.42	61.84	30.48
3	2.22	0.23	1.80	−8	−1	48	−5	17	19	18	14	83.33	106.58	96.49	48.46
2	2.89	0.20	2.57	−7	−5	51	−3	15	18	12	15	144.96	96.05	85.31	47.37
1	2.78	0.37	1.61	−8	−3	37	−3	14	16	12	11	121.27	71.93	108.55	51.97

Table 2
Measured maximum thickness of bottomsets, maximum thickness of topsets and differential sedimentation on shelf and basin for seismic units 1–4. MT_b - maximum thickness of bottomsets, MT_t - maximum thickness of topsets, As/Ab - differential sedimentation on shelf and basin.

Cross-Lines	MT_b (ms)				MT_t (ms)				As/Ab			
	SU1	SU2	SU3	SU4	SU1	SU2	SU3	SU4	SU1	SU2	SU3	SU4
8	104.82	70.39	96.71	52.19	0.00	53.95	59.65	29.82	0.00	0.77	0.62	0.57
7	113.60	86.84	112.50	50.44	0.00	54.82	100.66	30.04	0.00	0.63	0.89	0.60
6	102.19	55.48	107.24	66.45	0.00	42.11	95.83	36.62	0.00	0.76	0.89	0.55
5	96.71	60.96	110.31	57.24	0.00	42.11	92.54	35.75	0.00	0.69	0.84	0.62
4	96.93	59.43	94.52	49.34	0.00	53.95	93.42	46.27	0.00	0.91	0.99	0.94
3	89.91	58.99	104.82	39.91	0.00	60.31	89.47	30.92	0.00	1.02	0.85	0.77
2	85.31	59.21	105.26	39.04	0.00	43.86	87.06	31.80	0.00	0.74	0.83	0.81
1	71.27	55.04	92.98	66.45	0.00	36.62	97.59	34.43	0.00	0.67	1.05	0.52

The relationship between shelf-edge trajectories, stratal stacking patterns and sediment dispersal patterns in marine settings has been addressed by many previous researches (Johannessen and Steel, 2005; Henriksen et al., 2009, 2011; Gong et al., 2015a, b). In Qinnan Depression, an obvious relationship also exists. When shelf-edge trajectories are descending and stratal stacking patterns are progradational to downstepping (i.e. during the deposition of Seismic Unit 1 and 2), Sandy fans deposited on the basin floor as suggested by the high-amplitude properties of laterally continuous parallel seismic facies and corresponding high-amplitude RMS attributes in Figs. 5–7. And sandstone trajectories migrated in the same direction as shelf-edge trajectories (Fig. 9), indicating that the basinward boundary of sandstone prograde in basinward direction; When shelf-edge trajectories are ascending and stratal stacking patterns are progradational and aggradational (i.e. during the deposition of Seismic Unit 3), sandy fans mainly deposits on the slope and basin floor near the toe of slope, with small areas of sandy fans depositing on the shelf. And sandstone trajectories migrate in the opposite direction as shelf-edge trajectories, indicating that the basinward boundary of sandstone retrograde in landward direction (Fig. 9).

This kind of relationship could be the result of relative lake level change. When relative lake level falls, indicated as descending

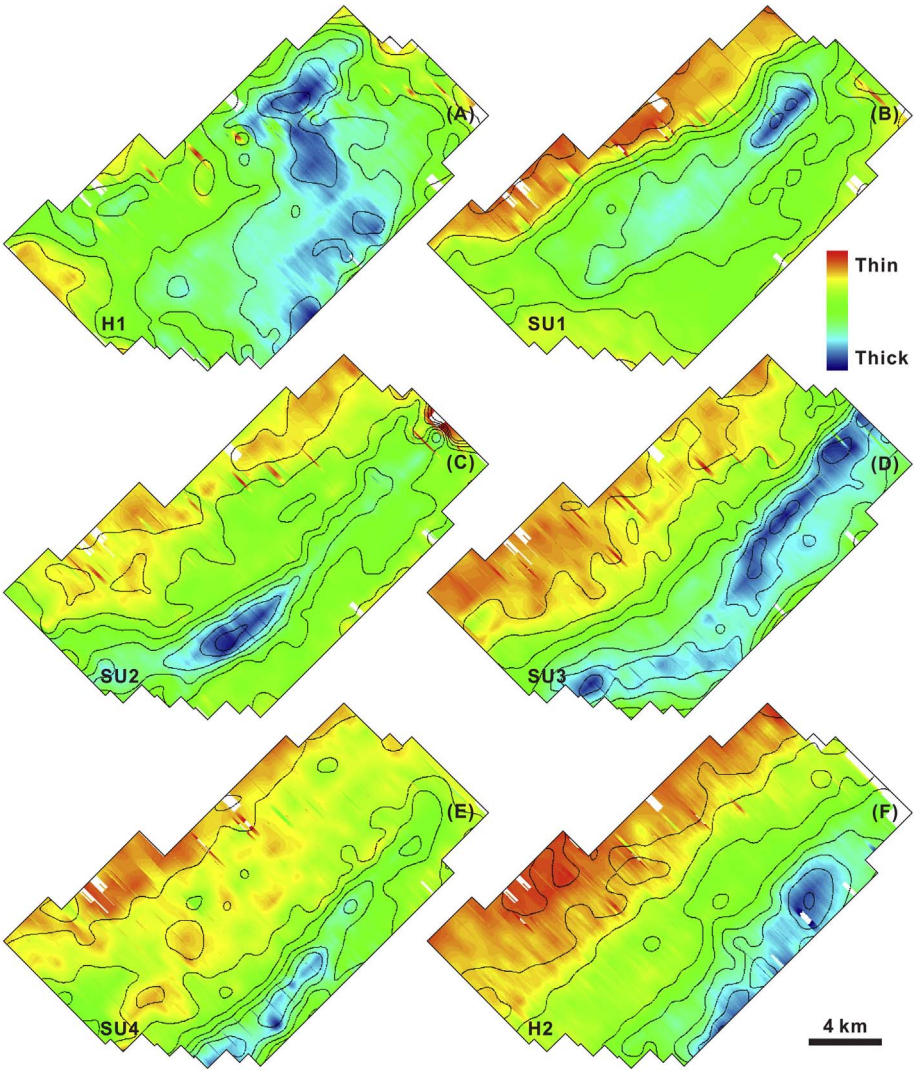

Fig. 8. Time Isochore maps of seismic units showing the locations of depocenter and their migration in each intervals. The locations of each intervals are shown in Fig. 4.

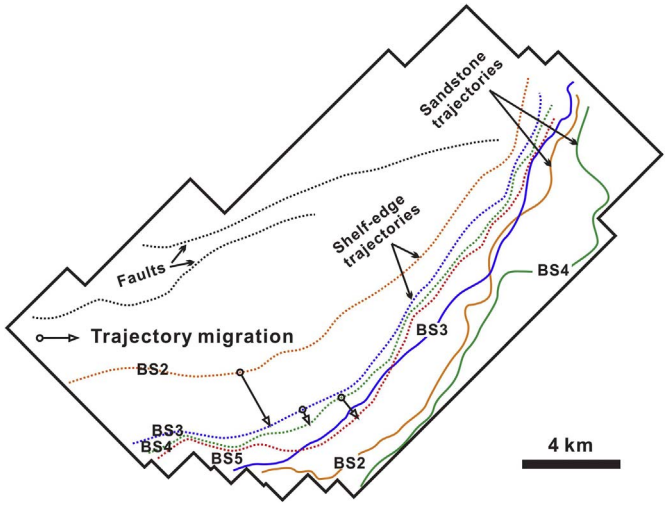

Fig. 9. A map view of shelf-edges migration from BS2 to BS5 (dashed lines) and sandstone trajectories extracted from RMS attribute maps in Fig. 7 (bold lines).

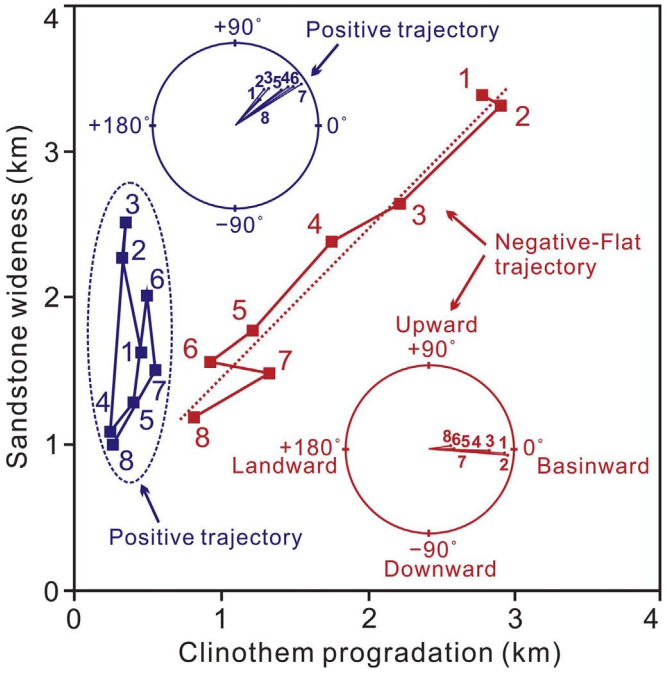

Fig. 10. Correlations between clinothem progradation and sandstone width for clinothems with descending shelf-edge trajectories in SU2 and clinothems with ascending trajectories in SU3. Clear positive correlation can be observed in SU2. No clear correlations can be observed in SU3.

trajectory, accommodation space on the shelf decreases and shelf-edge delta is forced to prograde, pushing sandy sediments to be transported to the basin floor. When relative lake level rises, indicated as ascending trajectory, accommodation space on the shelf increases and shelf-edge delta is forced to retrograde, and sediments would fill shelfal accommodation first before been transported to the slope and basin floor. It is noticeable that this relationship does not apply for SU4, possibly indicating external factors other than lake level change playing essential roles as discussed later.

Sediment supply could be another main factor affecting the relationship between shelf-edge trajectories, stratal stacking pattern and sandy sediment dispersal pattern. In particular, insufficient sediment supply would cause little or no sand delivered to the basin floor even during descending shelf-edge trajectories (e.g. the Høgsnyta clinoform complex documented by Plink-Bjorklund and Steel, 2002). Whereas very high sediment supply could bring significant sandy sediments to the deep-water areas even during ascending shelf-edge trajectories (e.g. the Lance-Fox Hills-Lewis shelf margins in southern Wyoming documented by Carvajal and Steel, and the Orinoco River shelf margins documented by Wood, 2000). Detailed investigation of sediment supply was not available in this study due to lack of absolute age control and insufficient data, while the relationship between shelf-edge trajectories and sediment dispersal patterns in the studied interval reflect relatively sufficient and constant sediment supply. The possible factors driving the changes in sediment supply in the studied interval could be local climate variations as discussed later.

Absolutely calculating volume of deep-water sandstone could be very difficult because of insufficient data and uncertainties. Several predictors have been proposed to predict volume of deep-water sandstone partitioning on the shelf and basin-floor, e.g. rates of shelf-edge progradation and ratios of shelf-edge progradation to aggradation proposed by Carvajal et al. (2009, 2012), and shelf-edge trajectory angles, clinoform heights, differential sedimentation on the shelf and basin proposed by Gong et al. (2015a, b). In this study, a new parameter, i.e. sandstone width measured on RMS attribute maps was also applied in combination with previous proposed predictors (progradation distances, shelf-edge trajectory angles) to establish possible relationship between volume of deep-water sandstone and shelf-edge trajectories and stratal stacking patterns.

In Seismic Units with descending shelf-edge trajectories (e.g. SU1, SU2 and parts of SU4), low shelf-edge trajectory angles (−10° - 0°) and greatest progradation distances (0.8–2.89 km) (Table 1) and ribbon-shaped high amplitude distribution on RMS maps (Fig. 7) is characteristic. All these observation indicates greater volume of sandstone delivered to deep-water area.

In Seismic Units with ascending shelf-edge trajectories (e.g. SU3 and parts of SU4), high shelf-edge trajectory angles (0–10°, 32–51°) and shortest progradation distances (0.18–0.58 km) (Table 1) and narrow medium-to high-amplitude strike elongate thread-shaped distribution on RMS maps (Fig. 7) is characteristic. All these observation indicates lesser volume of sandstone delivered to deep-water area.

Instead of quantitatively calculating volume of deep-water sandstone using mathematical equations (e.g. methods described by Petter et al., 2013), we used sandstone width, foreset dip and clinoform height to do rough estimation, as higher foreset dip and clinoform height favors greater sandy budget to be delivered to basin floor and greater accommodation in deep-water area. As summarized in Chapter 4.3 and 4.4, Seismic Units with descending shelf-edge trajectories have greater values of sandstone width, foreset dip and clinoform height than Seismic Units with ascending shelf-edge trajectories, further confirming the previous interpretation that greater volume of deep-water sandstone tend to form in front of descending shelf-edge trajectories. Within a single Seismic Unit with descending shelf-edge trajectories, sandstone width increase as trajectories decrease, possibly meaning greater volume of deep-water sandstone tend to be linked to lower shelf-edge trajectory angles.

5.2. *Differential tectonic subsidence controls lateral variability in shelf-edge trajectory, progradation and sediment dispersal*

Several mechanism have been brought up by previous studies on lateral variability in shelf-edge trajectory, progradation distances and sediment dispersal pattern, including local sediment supply variability (see Olariu and Steel, 2009 for discussion of point source sediment supply and Jones et al., 2015 for the proximity to a fluvial source), inherited basin physiology (see Henriksen et al., 2009 for discussion on influence of shelf width and Santra et al., 2013 for discussion on influence of basement high), influence of shelf-indenting canyons (Fongngern et al., 2015; Kertznus and Kneller, 2009), process regime (Johannessen and Steel, 2005; Dixon et al., 2012; Bourget et al., 2014; Jones et al., 2015) and local differential tectonic subsidence (Fongngern

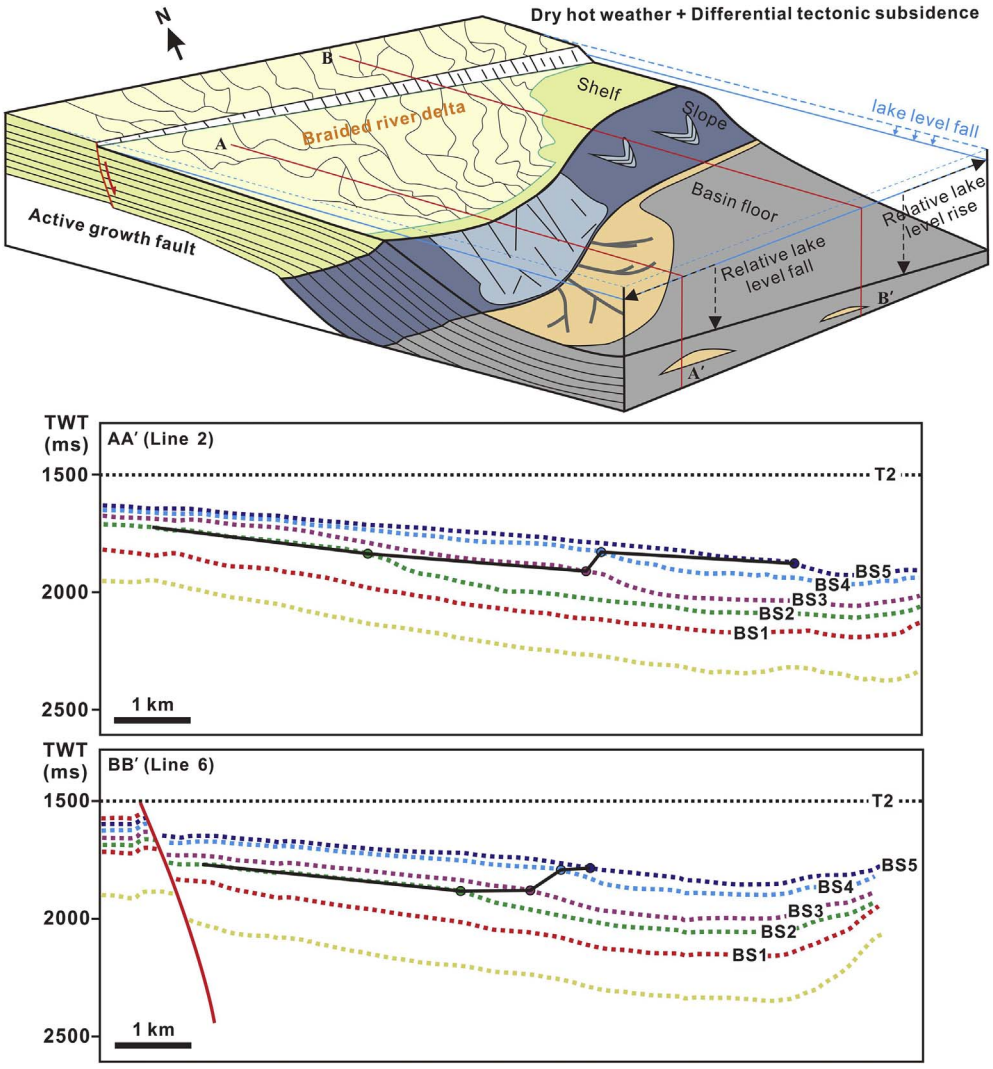

Fig. 11. (A) Depositional model of lacustrine clinoform growth controlled differential tectonic subsidence and local climate. During dry hot weather, the enhanced evaporation forces lake level to fall. Relative lake level rises in areas with great tectonic subsidence rate. Compared to areas with rising relative lake level, more sediments are supplied to the basin floor and greater progradation develops in areas with falling relative lake level; (B) two cross-sections show the associated variability in shelf-edge trajectories and progradation for SU2 and SU4.

et al., 2015).

The sediment input to the eastern sag in Qinnan depression mainly sourced from the adjacent Qinnan uplift and Liaoxi uplift in the form of wide-spread braided river deltas (Lai et al., 2007; Shi et al., 2014). Thus stark contrast process regimes along the shelf edge of the studied area is less plausible. Along-strike variation in sediment supply is possible. Qinnan uplift has the largest sediment source area comparing with the adjacent uplifts, and is clearly located to the N-NW of the basin. So that there might be a West to East decrease in direct sediment input along the paleo-shorelines. That could be one reason to explain the increased progradation trends to the West in their seismic data, with far less accommodation filled up to the East (lines 5–8) (Figs. 1 and 11).

Shelf-indenting canyons were not observed in seismic profiles, either because their dimensions were too shallow to be observed or they truly did not exist in the studied area. If shelf-indenting canyons did exist, abrupt change in progradation distances near the canyons should have been apparent, and sediments were supposed to be transported some distances away from the toe of slope. While the quantitative statistics of progradation distances acquired from 8 cross-lines suggest a gradual increase of progradation from northeast to southwest (Table 1). Hence the influence of shelf-indenting canyons could also be excluded.

Considering the active rifting stage during the deposition of Oligocene Dongying Formation, we attribute the lateral variability in trajectory, progradation and sediment dispersal to be partly caused by differential tectonic subsidence. The tectonic subsidence rate in Oligocene Dongying Formation was up to 80–150 m/Ma (Xie et al., 2007) and the dominant control of tectonic subsidence on sequence stratigraphy evolution in Bohai Bay basin has been suggested by Zhu et al. (2013), Xie et al. (2007) and Chen et al. (2012). In this study we address the influence of differential tectonic subsidence on lateral variability of sedimentation in Bohai Bay basin.

The influence of tectonic subsidence is most obvious during deposition of SU2 when the generally descending trajectory angles were gradually increasing from 0° in northeast to −5° southwest, and during SU4 when the trajectory is ascending in the northwest but descending in the southwest (Table 1). The progradation distances of SU2 and SU4 also follow certain patterns, as they increase from the least progradation distances of 0.797 km in SU2 and 0.299 km in SU4 in the northeast to the greatest of 2.895 km for SU2 and 2.567 km for SU4 in the southwest (Table 1).

The normal fault zone I and nearby secondary normal fault could be responsible for the variable tectonic subsidence (Fig. 3). As suggested in cross-line 6–8 where 3D seismic survey covers one of the normal faults, fault displacement across the footwall and the hanging wall of the growth fault in SU2 and SU4 is significant and tend to increase from line 8 to line 6 (Figs. 5B, 6A-6C). The controlling process is illustrated in Fig. 11. Normal faults movements were most active during the deposition of SU2 and SU4, with higher subsidence rate in the northeast than in the southwest. Normally, in a marine basin subsidence would result in relative sea level rise. While according to the model proposed by Sztanó et al. (2013), in lacustrine basins where volume of water mass is limited, if differential tectonic subsidence exist, relative lake

level would fall over high rate of tectonic subsidence, and would rise over areas of high subsidence rate. Hence, shelf margin prograded more distances when relative lake level falls a lot in high subsidence area, illustrated as high-angle descending trajectory, and prograded less when relative lake level falls a little or even rises in low subsidence area, illustrated as low-angle descending and ascending trajectory (Fig. 11). Variable tectonic subsidence rates also affect depocenter migration shown in time isochore maps. As high progradation distances expanded the extent of foresets area in SU2 and SU4, the depocenter migrated to southwest during SU2 and SU4 (Fig. 8).

5.3. Is climate change a driving force for lacustrine clinoform growth?

Paleoclimate is believed to be the major controlling factor driving the formation of lacustrine sequence stratigraphy. Although detailed investigation on climate control throughout the study interval is not available for lack of core samples, geochemical analysis and age control, the trends of shelf-edge trajectories and sediment dispersal patterns could still reflect climate signal. Combing with previous studies in paleoclimate, we discuss herein whether the long-term global climate change and short-term local climate variation have acted as a driving force for lacustrine clinoform growth.

The control of global climate on marine clinoform growth and basin-floor fans deposition has been investigated by many researchers (Blum and Hattier-Womack, 2009; Sømme et al., 2009; Kertznus and Kneller, 2009; Salazar et al., 2015; Gong et al., 2016a). But the documentations of global climate control on lacustrine clinoform growth are rare. We suggest the general trend of global climate change could have affected lacustrine clinoform growth.

Early Oligocene was marked by rapid cooling and long-term sea-level fall by 55 m with short-term fluctuating sea-level rise and fall (Zachos et al., 2001). Palynological assemblages (Wang et al., 2005) suggested that the paleoclimate of North China mainland, especially in Bohai Bay Basin, was also influenced by the global cooling trend during Early Oligocene. Such global cooling trend could have driven the long-term relative lake level change and clinoform growth in two ways. Firstly, during general arid and cold Oligocene icehouse periods, coupled to decreasing vegetation cover, the production of coarse sediments would most likely increased due to the enhanced physical erosion. Secondly, descending trajectory with great progradation predominate in the study interval, meaning the relative lake level showed a general falling trend, coinciding with the long-term sea level falling trend in Oligocene.

Compared with marine settings, local climatic signatures is believed to strongly influence base-level variations and rate of sediment supply in lacustrine basins. The studies of Sztanó et al. (2013) in Pannonian lake basin suggested that local cyclic climate changes, mainly the climate cycle of hot dry and cold humid, controlled relative lake level change and sediment supply, hence the formation of shelf-edge trajectories and the deposition of basin-floor fans in lacustrine settings. In Qinnan Depression, we also observed possible trends between local climate and relative lake level change, progradation and basin-floor fan deposition. Pollen analysis (Wu et al., 2012) suggested that the paleoclimate of Oligocene Dongying formation showed obvious cyclicity of hot dry and cold humid weather in Bohai Bay basin. We suggest that local hot dry weather would have resulted in enhanced evaporation leading to relative lake level fall and descending shelf-edge trajectories, and enhanced physical erosion leading to increasing sediment supply bypassing to deep water area and thus the deposition of large basin-floor fan. It therefore explains why large basin-floor fan formed in clinoforms with descending shelf-edge trajectories and great progradation.

5.4. Evolution stages of shelf-edge trajectory in the Qinnan depression

Based on the above results and discussion, the lacustrine margin evolution can be subdivided into three stages. Each evolution stage show distinct relative lake level trend, stratal stacking patterns, sediment dispersal patterns and influence of tectonic subsidence and local climate.

The first stage comprises SU1 and SU2, during which local climate might play a major role in controlling lake-margin evolution. Dry hot climate led to intense evaporation and great physical weathering rate, causing relative lake level show a falling trend and substantial amount of coarse sediment supply, indicated by generally falling trajectory and associated long progradation distances and big area of sandy fan deposition. Differential tectonic subsidence also had minor effects, as shown in various trajectory angles and progradation in northeast and southwest region of SU2, but it does not overrun the domination of local climate.

The second stage comprises SU3, when humid and cold climate leads to intense precipitation and less physical weathering rate. As a result, relative lake level rose and sediment supply decreased. The various progradation distances in SU2 formed lacustrine shelf with various width, which further influenced the transportation of sandy sediments, thus the basin-floor fan distribution area.

The third stage comprises SU4. Differential tectonic subsidence could have the dominate role in controlling lacustrine margin evolution. Decreasing rates of subsidence rate from northeast region to southwest region caused shelf-edge trajectory angles to ascend in northeast and descend in southwest (Fig. 11).

6. Conclusion

Based on interpretation of seismic lines and seismic attribute maps, associated with calculation of quantitative parameters such as shelf-edge trajectory angles, progradation distances, forest dip, clinoform height, maximum thickness of topsets and bottomsets and differential sedimentation on shelf and basin, four conclusions can be drawn.

1. Four seismic units are identified. Four types of shelf-edge trajectories and the associated stratal stacking patterns can be recognized. Steeply descending trajectory with progradational and down-stepping stratal stacking pattern can be observed in Seismic Unit1, slightly descending to flat trajectory with aggradational and progradational stratal stacking pattern can be observed in Seismic Unit2, and steeply ascending trajectory with aggradational and progradational stratal stacking pattern can be observed in Seismic Unit 3. Both slightly ascending trajectorires and slightly descending to flat trajectorires with aggradational and progradational stratal stacking pattern can be observed in Seismic Unit4. Greater volume of sandstone in deep-water area tends to develop in seismic units with descending shelf-edge trajectory angles and tends be linked to lower shelf-edge trajectory angles.
2. Differential tectonic subsidence and along-strike variation in sediment supply might have controlled lateral variability in trajectory, progradation and sediment dispersal. The normal fault zone I and nearby secondary normal fault could be responsible for the variable tectonic subsidence. Differential subsidence in different regions might cause variable relative lake level change and variable progradation distances to occur. Variable tectonic subsidence rates also affect depocenter migration. As high progradation distances expanded foresets thickness, the depocenter migrated to southwest. Qinnan uplift has the largest sediment source area comparing with the adjacent uplifts, and is clearly located to the N-NW of the basin. So that a West to East decrease in direct sediment input along the paleo-shorelines might also have influenced the observed lateral variability.
3. Evolution of shelf-edge trajectory have been subdivided into three stages. The first stage comprises SU1 and SU2, during which local climate might play a major role in controlling lake-margin evolution. Dry hot climate leads to generally falling relative lake level and

associated long progradation distances and big area of sandy basin-floor fan deposition. The second stage comprises SU3, when humid and cold climate lead to relative lake level rise and sediment supply decreases. The various progradation distances in SU2 form lacustrine shelf with various width, which further influenced the transportation of sands, thus the distribution area of basin floor fan. The third stage comprises SU4. Differential tectonic subsidence could have the dominate role in controlling lacustrine margin evolution. Decreasing subsidence rate from northeast region to southwest region caused trajectory angles to ascend in northeast and descend in southwest.

Acknowledgements

This research was supported by the National Natural Science Foundation of China (41690131, 41690134), National Science & Technology Specific Project (2016ZX05024-003-008), Strategic Priority Research Program of the Chinese Academy of Sciences (XDA14010302) and the Fundamental Research Funds for the Central Universities, China University of Geosciences (Wuhan) (CUG160605). We thank MPG Editor Dr. Istvan Csato and reviewer Dr. Julien Bourget for their thorough and critical reviews and suggestions to improve the manuscript.

References

Blum, M.D., Hattier-Womack, J., 2009. Climatic change, sea-level change and fluvial sediment supply to deepwater depositional systems. In: In: Kneller, B., Martinsen, O.J., McCaffrey, B. (Eds.), External Controls on Deep-water Depositional Systems 92. Society of Economic Paleontologists and Mineralogists Special Publication, pp. 15–39.

Bourget, J., Ainsworth, R.B., Thompson, S., 2014. Seismic stratigraphy and geomorphology of a tide or wave dominated shelf-edge delta (NW Australia): process-based classification from 3D seismic attributes and implications for the prediction of deep-water sands. Mar. Petrol. Geol. 57, 359–384.

Bullimore, S., Helland-Hansen, W., Henriksen, S., et al., 2008. Shoreline trajectory and its impact on coastal depositional environments: an example from Upper Cretaceous Mesaverde Group, NW Colorado. In: In: Hampson, G.J., Steel, R.J., Burgess, P., Dalrymple, R.W. (Eds.), Recent Advances in Models of Siliciclastic Shallow-Marine Stratigraphy, vol 90. SEPM Special Publication, pp. 209–236.

Bullimore, S.A., Helland-Hansen, W., 2009. Trajectory analysis of the lower Brent Group (Jurassic), Northern North Sea: contrasting depositional patterns during the advance of a major deltaic system. Basin Res. 21, 559–572.

Carroll, A.R., Bohacs, K.M., 1999. Stratigraphic classification of ancient lakes: balancing tectonic and climatic controls. Geology 27, 99–102.

Carvajal, C., Steel, R., 2006. Thick turbidite successions from supply-dominated shelves during sea-level highstand. Geology 34, 665–668.

Carvajal, C., Steel, R., Petter, A., 2009. Sediment supply: the main driver of shelf-margin growth. Earth Sci. Rev. 96, 221–248.

Catuneanu, O., Abreu, V., Bhattacharya, J.P., et al., 2009. Towards the standardization of sequence stratigraphy. Earth Sci. Rev. 92, 1–33.

Chen, S., Wang, H., Zhou, L.H., Huang, C.Y., Wang, J.H., Ren, P.G., Xiang, X.M., 2012. Sequence thickness and its response to episodic tectonic evolution in Paleogene Qikou Sag, Bohaiwan Basin. Acta Geol. Sin. 86 (5), 1077–1092.

Deibert, J.E., Benda, T., Loseth, T., Schellpeper, M., Steel, R.J., 2003. Eocene clinoform growth in front of a storm-wave-dominated shelf, Central Basin, Spitsbergen: no significant sand delivery to deepwater areas. J. Sediment. Res. 73, 546–558.

Dixon, J.F., Steel, R.J., Olariu, C., 2012. Shelf-edge delta regime as a predictor of the deepwater deposition. J. Sediment. Res. 82, 681–687.

Fongngern, R., Olariu, C., Steel, R.J., et al., 2015. Clinoform growth in a Miocene, Paratethyan deep lake basin: thin topsets, irregular foresets, and thick bottomsets. Basin Res. 28, 77–795.

Ge, T., Chen, Y., 1993. Liaohe Oilfield. Petroleum Geology of China III. Petroleum Industry Press, Beijing, pp. 237 (in Chinese).

Gong, C., Wang, Y., Pyles, D., et al., 2015a. Shelf-edge trajectories and stratal stacking patterns: their sequence-stratigraphic significance and relation to styles of deep-water sedimentation and amount of deep-water sandstone. AAPG Bulletin 99, 1211–1243.

Gong, C., Wang, Y., Steel, R., et al., 2015b. Growth styles of shelf-margin clinoforms: prediction of sand- and sediment-budget partitioning into and across the shelf. J. Sediment. Res. 85, 209–229.

Gong, C., Steel, R.J., Wang, Y., et al., 2016a. Grain size and transport regime at shelf edge as fundamental controls on delivery of shelf-edge sands to deepwater. Earth Sci. Rev. 157, 32–60.

Gong, C., Steel, R.J., Wang, Y., et al., 2016b. Shelf-margin architecture variability and its role in source-to-sink sediment budget partitioning. Earth Sci. Rev. 154, 72–101.

Hao, F., Zou, H.Y., Gong, Z.S., Deng, Y.H., 2007. Petroleum migration and accumulation in the Bozhong sub-basin, Bohai Bay basin, China: significance of preferential petroleum migration pathways (PPMP) for the formation of large oilfields in lacustrine fault basins. Mar. Petrol. Geol. 24, 1–13.

Hao, F., Zhou, X.H., Zhu, Y.M., Bao, X.H., Yang, Y.Y., 2009. Charging of the Neogene Penglai 19-3 field, Bohai Bay basin, China: oil accumulation in a young trap in an active fault zone. AAPG Bulletin 93, 155–179.

Helland-Hansen, W., Gjelberg, J.G., 1994. Conceptual basis and variability in sequence stratigraphy; a different perspective. Sediment. Geol. 92, 31–52.

Helland-Hansen, W., Hampson, G., 2009. Trajectory analysis: concepts and applications. Basin Res. 21, 454–483.

Helland-Hansen, W., Martinsen, O.J., 1996. Shoreline trajectories and sequences; description of variable depositional-dip scenarios. J. Sediment. Res. 66, 670–688.

Henriksen, S., Hampson, G.J., Helland-Hansen, W., et al., 2009. Shelf edge and shoreline trajectories, a dynamic approach to stratigraphic analysis. Basin Res. 21, 445–453.

Henriksen, S., Helland-Hansen, W., Bullimore, S., 2011. Relationships between shelf-edge trajectories and sediment dispersal along depositional dip and strike: a different approach to sequence stratigraphy. Basin Res. 23, 3–21.

Hou, G.T., Qian, X.L., Cai, D.S., 2001. The tectonic evolution of Bohai Basin in Mesozoic and Cenozoic time. Acta Sci. Nat. Universitatis Pekinensis 37, 845–851 (in Chinese with English abstract).

Huang, H.P., Pearson, M.J., 1999. Source rock palaeoenvironments and controls on the distribution of dibenzothiophenes in lacustrine crude oils, Bohai Bay basin, eastern China. Org. Geochem. 30, 1455–1470.

Johannessen, E.P., Steel, R.J., 2005. Shelf-margin clinoforms and prediction of deepwater sands. Basin Res. 17, 521–550.

John, A., Lake, L.W., Torres-Verdin, C., Srinivasan, S., 2005. Seismic facies identification and classification using simple statistic. In: SPE Annual Technical Conference and Exhibition, (Dallas, SPE).

Jones, G.E.D., Hodgson, D.M., Flint, S.S., 2015. Lateral variability in clinoform trajectory, process regime, and sediment dispersal patterns beyond the shelf-edge rollover in exhumed basin margin-scale clinothems. Basin Res. 27, 657–680.

Kertznus, V., Kneller, B., 2009. Clinoform quantification for assessing the effects of external forcing on continental margin development. Basin Res. 21, 738–758.

Lai, W.C., Xu, C.G., Wang, X.G., Wang, C.Z., Liu, F.P., 2007. A study on Paleogene sequence stratigraphy and sedimentary systems and a discussion on hydrocarbon exploration directions in Qinnan depression. China Offshore Oil Gas 19 (5), 300–305 (in Chinese with English abstract).

Mellere, D., Plink-Björklund, P., Steel, R.J., 2002. Anatomy of shelf-edge deltas on prograding Eocene shelf margin, Spitsbergen. Sedimentology 49, 1181–1206.

Mitchum Jr., R.M., Vail, P.R., Thompson III, S., 1977. Seismic stratigraphy and global changes of sea-level, part 2: the depositional sequence as a basic unit for stratigraphic analysis. In: In: Payton, C.E. (Ed.), Seismic Stratigraphy–Applications to Hydrocarbon Exploration, vol. 26. AAPG Memoir, pp. 53–62.

Munteanu, I., Matenco, L., Dinu, C., Cleotingh, S., 2012. Effects of large sea-level variations in connected basins: the Dacian-Black Sea system of the Eastern Paratethys. Basin Res. 24, 583–597.

Muto, T., Steel, R.J., 1997. Principles of regression and transgression: the nature of the interplay between accommodation and sediment supply: perspectives. J. Sediment. Res. 67, 994–1000.

Muto, T., Steel, R.J., Swenson, J.B., 2007. Autostratigraphy: a framework norm for genetic stratigraphy. J. Sediment. Res. 77, 2–12.

Olariu, C., Steel, R.J., 2009. Influence of point-source sediment-supply on modern shelf-slope morphology: implications for interpretation of ancient shelf margins. Basin Res. 21, 484–501.

Petter, A.L., Steel, R.J., 2006. Hyperpycnal flow variability and slope organization on an Eocene shelf margin, Central Basin, Spitsbergen. AAPG Bulletin 95, 1451–1472.

Petter, A.L., Steel, R.J., Mohrig, D., Kim, W., Carvajal, C., 2013. Estimation of the palaeoflux of terrestrial-derived solids across ancient basin margins using the stratigraphic record. GSA Bulletin 125, 578–593.

Plink-Björklund, P., Steel, R., 2002. Sea-level fall below the shelf edge, without basin-floor fans. Geology 30, 115–118.

Ryan, M.C., Helland-Hansen, W., Johannessen, E.P., et al., 2009. Erosional vs. accretionary shelfmargins: the influence of margin type on deepwater sedimentation: an example from the Porcupine Basin, offshore western Ireland. Basin Res. 21, 676–703.

Salazar, M., Moscardelli, L., Wood, L., 2015. Utilising clinoform architecture to understand the drivers of basin margin evolution: a case study in the Taranaki Basin, New Zealand. Basin Res. 1–26.

Santra, M., Steel, R.J., Olariu, C., et al., 2013. Stages of sedimentary prism development on a convergent margin — Eocene Tyee Forearc Basin, coast range, Oregon, USA. Global Planet. Change 103, 207–231.

Shi, W.L., Li, H.Y., Mao, L., Yang, H.F., Chen, L.X., Yu, H.B., 2014. Hydrocarbon geological characteristics and exploration potential of Qinnan depression in offshore area of Bohai Sea. China Pet. Explor. 19 (5), 32–40 (in Chinese with English abstract).

Sømme, T.O., Helland-Hansen, W., Granjeon, D., 2009. Impact of eustatic amplitude variations on shelf morphology, sediment dispersal, and sequence stratigraphic interpretation: icehouse versus greenhouse systems. Geology 37, 587–590.

Steel, R.J., Crabaugh, J., Schellpeper, M., Mellere, D., Plink-Bjorklund, P., Deibert, J., Løseth, T.M., 2000. Deltas versus rivers on the shelf edge: their relative contributions to the growth of shelf margins and basin-floor fans (Barremian and Eocene, Spitsbergen). In: Weimer, P. (Ed.), Deep-water Reservoirs of the World. Gulf Coast Section SEPM Foundation 20th Annual Research Conference, pp. 981–1009 Houston, Texas.

Steel, R.J., Olsen, T., 2002. Clinoforms, clinoform trajectories and deepwater sands. In: Armentrout, J.M., Rosen, N.C. (Eds.), Sequence Stratigraphic Models for Exploration and Production: Evolving Models and Application Histories. GCSSEPM Special Publication, pp. 367–381.

Steel, R.J., Carvajal, C., Petter, A., et al., 2008. The growth of shelves and shelf margins. In: In: Hampson, G.J., Steel, R.J., Burgess, P., Dalrymple, R.W. (Eds.), Recent

Advances in Shallow-Marine Stratigraphy: Perspectives and Applications, vol 90. SEPM Special Publication, pp. 7–71.
Sztanó, O., Szafián, P., Magyar, I., et al., 2013. Aggradation and progradation controlled clinothems and deep-water sand delivery model in the Neogene Lake Pannon, Makó Trough, Pannonian basin, SE Hungary. Global Planet. Change 103, 149–167.
Uhrin, A., Sztanó, O., 2011. Water-level changes and their effect on deepwater sand accumulation in a lacustrine system: a case study from the Late Miocene of western Pannonian Basin, Hungary. Int. J. Earth Sci. 101 (5), 1427–1440.
Wang, B., Qian, K., 1992. Geology Research and Exploration Practice in the Shengli Petroleum Province. Petroleum University Press, Dongying, pp. 319 (in Chinese).
Wang, X.M., Wang, M.Z., Zhang, X.L., 2005. Palynology assemblages and paleoclimatic character of the late Eocene to the early Oligocene in China. Earth Sci. J. China Univ. Geosci. 30 (3), 309–316.
Wood, L., 2000. Chronostratigraphy and tectonostratigraphy of the Columbus Basin, eastern offshore Trinidad. AAPG Bull. 84 (12), 1905–1928.
Wu, W., Lin, C.S., Zhou, X.H., Li, Q., Xing, Z.C., Yan, Yu, 2012. Paleoclimate evolution and its influence on lake level changes of Paleogene Dongying epoch in Liaodong Bay, East China. J. China Univ. Pet. 36 (1), 33–46 (in Chinese with English abstract).
Xie, X.N., Cui, T., Müller, D., Guo, X.R., Liu, X.F., Cheng, Zhang, 2007. Subsidence history and forming mechanism of anomalous tectonic subsidence in the Bozhong depression, Bohaiwan basin. Sci. China Earth Sci. 50 (9), 1310–1318.
Xu, S., Hao, F., Xu, C., Zou, H., Tian, J., 2014. Tracing migration pathways by integrated geological, geophysical and geochemical data: a case study from the JX1-1 oil field, Bohai Bay basin, China. AAPG Bulletin 98 (10), 2109–2129.
Xu, S., Hao, F., Xu, C., Wang, Y., Zou, H., Gong, C., 2015. Differential compaction faultsand their implications for fluid expulsion in the northern Bozhong Subbasin, Bohai Bay Basin, China. Mar. Petrol. Geol. 63, 1–16.
Xu, S., Hao, F., Xu, C., Zou, H., Quan, Y., 2016. Oil migration through preferential petroleum migration pathway (PPMP) and polycyclic faults: a case study from the Shijiutuo Uplift, Bohai Bay basin, China. Mar. Petrol. Geol. 73, 539–553.
Zachos, J., Pagani, M., Sloan, L., Thomas, E., Billups, K., 2001. Trends, rhythms, and aberrations in global climate 65 Ma to present. Science 292, 686–693.
Zhu, H.T., Zeng, H.L., Liu, K.Y., 2013. A quantitative simulation study of asymmetrical tectonic subsidence control on non-synchronous sequence stacking patterns of Eocene lacustrine sediments in Bohai Bay Basin, China. Sediment. Geol. 294, 328–341.